

Preliminary thermo-mechanical assessment of the Top Cap region of the Water-Cooled Lead-Ceramic Breeder Breeding Blanket alternative concept

S. Giambrone^{a,*}, I. Catanzaro^a, G. Bongiovi^a, P.A. Di Maio^a, E. Vallone^a, P. Arena^b,
F.A. Hernández^c, I. Moscato^c, G.A. Spagnuolo^c, P. Chiovaro^a, M. Giardina^a, A. Quartararo^a,
E. Tomarchio^a

^a Department of Engineering, University of Palermo, Viale delle Scienze Ed. 6, 90128, Palermo, Italy

^b Department of Fusion and Nuclear Safety Technology, ENEA, C.R. Brasimone, 40032, Camugnano (BO), Italy

^c Fusion Technology Department – Programme Management Unit, EUROfusion Consortium, Boltzmannstraße 2, 85748, Garching, Germany

ARTICLE INFO

Keywords:

WLCB
DEMO
Breeding blanket
Top cap
Thermomechanics
FEM analysis

ABSTRACT

The Water-Cooled Lead Lithium (WCLL) and the Helium-Cooled Pebble Bed (HCPB) Breeding Blanket (BB) concepts are the two candidates currently poised to be chosen as the driver blanket for the EU DEMO reactor. Nevertheless, new variants are emerging with the aim of overtaking the potential showstoppers arisen during the WCLL and HCPB BB pre-conceptual design phase. Then, an intense campaign of exploratory studies has been launched in EU to investigate the potential performances of such alternative concepts. Among them, the Water-Cooled Lead-Ceramic Breeder (WLCB) BB concept is one of the most promising. It has been conceived as a trade-off (i.e. a hybrid concept) between WCLL and HCPB BB concepts, trying to take and integrating the best features of both. Since in the reference WCLL geometric layout the Top Cap (TC) region was identified as particularly critical from thermal and mechanical standpoints, so requiring specific design studies, also in the WLCB conceptual design activities a dedicated campaign of analysis has been necessary to preliminarily size the TC region components. Hence, in this paper, the preliminary thermo-mechanical assessment of the TC region of the WLCB BB alternative concept is presented. First, an initial geometric layout has been set-up on the basis of the main features of the reference WCLL BB TC region. Then, thermal analysis under nominal conditions has been performed and the results have shown that modifications were necessary to ensure the compliance with the thermal requirements of the structural material. Finally, once obtained an acceptable geometric layout, mechanical analyses were carried out in order to verify the fulfilment of the RCC-MRx structural design criteria, also considering an off-normal load case. The results showed that this variant is very promising in terms of structural behaviour, whereas further design iterations are necessary to lower the temperature of the breeder zone.

1. Introduction

The Water-Cooled Lead Lithium (WCLL) and the Helium-Cooled Pebble Bed (HCPB) Breeding Blanket (BB) concepts are the two candidates currently poised to be chosen as the driver blanket for the EU DEMO reactor. Nevertheless, new variants are emerging with the aim of overtaking the potential showstoppers arisen during the WCLL and HCPB BB pre-conceptual design phase [1]. In this context, the Water-Cooled Lead-Ceramic Breeder (WLCB) BB concept is one of the most promising [2]. It has been conceived as a trade-off (i.e. an hybrid concept) between WCLL and HCPB BB concepts, trying to take and integrate the best features of both. Considering that in the geometric layout of the reference WCLL, the Top Cap (TC) region was identified

as particularly critical from a thermal and mechanical point of view [3], a structural analysis campaign was carried out on the same area of the WLCB Central Outboard Blanket (COB) in order to define its preliminary design. Hence, in this work, the adopted methodology, the models set-up and the results obtained are reported and critically discussed, paving the way for future and more detailed assessments.

2. The WLCB top cap geometric configuration

The WLCB BB concept foresees water as coolant, with a pressure of 15.5 MPa and an inlet–outlet temperature equal to 285–325 C, and pebble beds of Advanced Ceramic Breeder (ACB) as breeder crossed by gaseous helium as purge gas. In addition, molten lead acts as neutron

* Corresponding author.

E-mail address: salvatore.giambrone04@unipa.it (S. Giambrone).

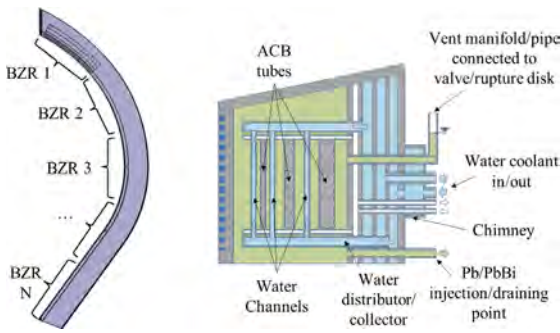


Fig. 1. WLCB BZR cooling system qualitative scheme.

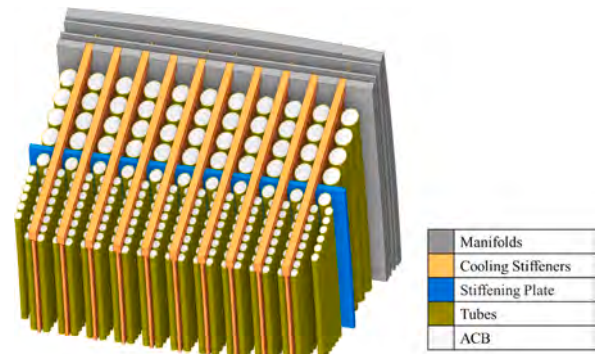


Fig. 3. WLCB TC ver. 0 internals.

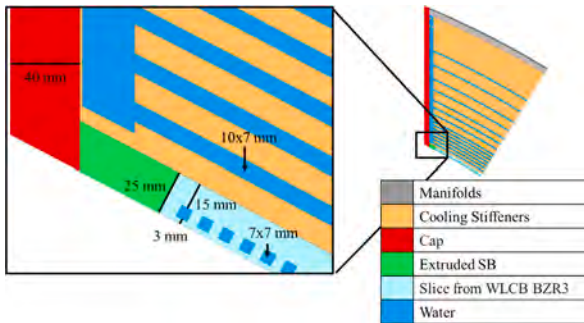


Fig. 2. WLCB TC ver. 0.

multiplier, as described in [2]. A WLCB COB segment can be subdivided into a certain number of Breeder Zone Region (BZR), as shown in Fig. 1, distributed along its poloidal length.

Two plates close the segment at the top and bottom regions, the caps. Each BZR is constituted by an external steel structure made in Eurofer named Segment Box (SB), which is composed by First Wall (FW), covered with 2 mm of Tungsten, and Side Wall (SW). In the FW-SW region, square cooling channels are located. The SB is internally reinforced by means of some Cooling Stiffeners (CSs), namely poloidal-radial plates equipped with square cooling channels aimed at cooling the breeding zone, and additional poloidal-toroidal stiffening plates to withstand an in-box LOCA. A set of tubes, aimed at housing the ACB and the purge gas, are located between the CSs, immersed in the molten lead.

With the aim of studying the TC region, located in the BZR1, a proper geometric model has been created. To this purpose, starting from the provided BZR3 region geometric layout, a portion encompassing 30 FW-SW cooling channels has been cut and properly moved to the same position as in the reference WCLL TC region [4]. Then, SB, CSs, manifolds and tubes have been extruded in order to place the TC plate perpendicular to X axis, as the reference position, in order to obtain a first attempt geometric layout called TC ver.0, showed in Fig. 2.

In this preliminary version, the TC, with a thickness of 40 mm, is full and no cooling system is foreseen. The adjacent BZR, with a 25 mm thick FW, is equipped with 7 × 7 mm square channels. Instead, as to the CSs, 140 channels of 10 × 7 mm are foreseen. In Fig. 3 a detail of the TC ver.0 internals is reported. In particular, 227 tubes with a thickness of 13 mm, filled with ACB, are located among the 10 CSs, and a 20 mm thick stiffening plate is present too. It has to be noted that no purge gas collectors and manifolds have been considered at this stage.

3. The adopted methodology

The design of the WLCB TC region has been performed following a “design by analysis” approach. In particular, in a first phase, TC ver.0



Fig. 4. Heat flux onto Tungsten layer.

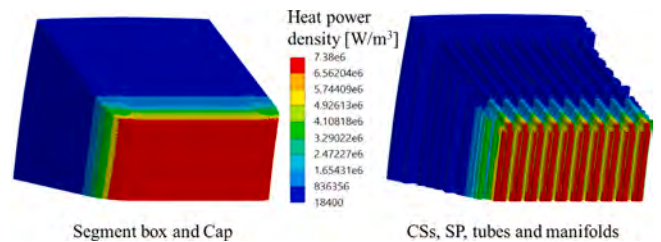


Fig. 5. Volumetric heat power density on Eurofer.

has been assessed from the thermal point of view. Then, some design modifications have been implemented in two different steps in order to finally obtain a geometric configuration able to withstand the thermal requirement (i.e. maximum temperature in the Eurofer steel lower than 550 C) under the nominal loading conditions. Afterwards, such configuration, called TC ver.2, has been investigated from the structural point of view under selected (normal and off-normal) loading scenarios, in order to check the fulfilment of the RCC-MRx design criteria.

4. Assessment of the boundary conditions for the thermal analyses

This section reports the evaluation of the loads and boundary conditions implemented in all the thermal analyses carried out.

4.1. Heat flux

A non-uniform value of heat flux coming from plasma has been imposed onto the Tungsten surface. A value of 0.24 MW/m² has been applied onto the straight Tungsten surface, whereas a cosine-dependent law decreasing to 0 has been assumed to the bend ones (Fig. 4).

4.2. Power density

With the aim of taking into account the deposited nuclear power density, a non-uniform spatial distribution of heat power volumetric

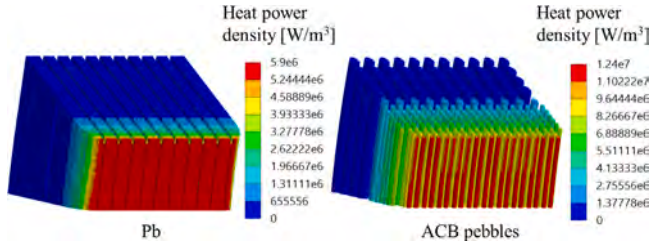


Fig. 6. Volumetric heat power density on lead and ACB.

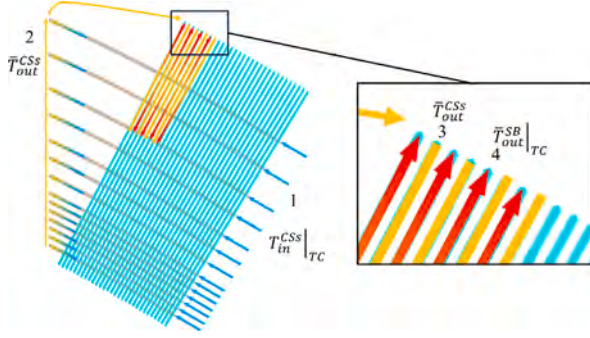


Fig. 7. Coolant flow path within CSs and SB channels.

density has been applied to the components, differentiating properly for tungsten, Eurofer, Pb and ACB [5]. Since the provided power density 3D spatial distributions have been calculated for the equatorial WLCB region, the corresponding values at the BZR1 region have been obtained by scaling the provided distributions with the ratio of the corresponding neutron wall loading average values, as done for the design analysis of the reference WCLL TC [3]. In Figs. 5 and 6 the so obtained power density spatial distributions are reported.

4.3. Convective conditions

A forced convective heat transfer condition between coolant and water-wetted surfaces has been imposed. In this regard, in order to reproduce the coolant flow, the “thermal fluids” approach, available in the Ansys Steady-State Thermal module, has been adopted. This allows representing the fluid flowing within each channel by means of a 1-D body. Then, it is discretized and coupled to the nodes of the channel surfaces by means of a convective boundary condition. In order to properly impose the load, the user has to provide the Mass Flow Rate (MFR), the Heat Transfer Coefficient (HTC) and the inlet bulk temperature. As a result, the bulk temperature profile along the thermal fluid is obtained and used in the calculation.

In order to retrieve the input data, the WLCB COB segment has to be evaluated from a design point of view. In this regard, as reported in Fig. 1, and in [2], it has to be noted that, differently from the reference WCLL BB, in this case only one hydraulic loop is responsible for the segment cooling.

As a consequence, the coolant enters through the system’s inlet manifold at 285 C ($T_{in}^{CSs}|_{TOT}$). Then it flows inside the CSs in co-current and mixes exiting in a dedicated manifold reaching a certain mean temperature that has to be evaluated (\bar{T}_{out}^{CSs}). Finally, it goes inside the FW-SW channels in counter-current and exits in the system’s outlet manifold at 325 C ($T_{out}^{SB}|_{TARGET}$). Since the water enters the CSs from the bottom of the BZR1 (Fig. 1), its temperature entering the portion of the CSs reproduced in the model ($T_{in}^{CSs}|_{TC}$, Fig. 7) is also unknown.

Hence, the following procedure has been purposely conceived with the aim of determining all the unknown (MFR per channel, HTC, $T_{in}^{CSs}|_{TC}$ and \bar{T}_{out}^{CSs}) necessary to properly characterize the model from

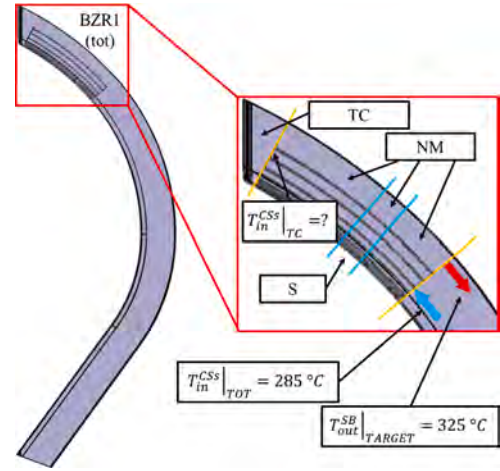


Fig. 8. Detail of the convective condition calculation.

the thermal-hydraulic standpoint, allowing the imposition of the above said forced convective heat transfer condition and of further thermal boundary conditions within the manifolds. The procedure starts considering that, in analogy to the other WCLL BB variants, one can be assumed that the WLCB COB segment is divided into 5 BZR1s. Hence, once known the pitch between the SB channels and the total length of the segment, it can be assumed that each BZR1 houses 212 SB channels (n_{tot}^{SB}). Considering that the model of the TC region encompasses 30 SB channels (n_{TC}^{SB}), it is possible deducing that the Not Modelled (NM) BZR1 portion (namely the BZR1 region between the yellow lines in Fig. 8) houses 212 - 30, i.e. 182, cooling channels (n_{NM}^{SB}).

At this point, to evaluate the CSs water inlet temperature in the modelled TC region, the thermal power exchanged in the NM part of BZR1 must be estimated. To this purpose, if one considers a Slice (S) of the NM portion (Fig. 8) housing 30 SB channels, one can obtain the volumetric ratio between NM and S regions (V_{NM}/V_S), which is equal to 182/30 \approx 6. Therefore, a dedicated steady-state thermal analysis of the above mentioned Slice has been performed with the same power density and heat flux already shown but with “dummy” convective conditions, in order to evaluate the heat power removed by the coolant ($\dot{Q}_S = \dot{Q}_S^{SB} + \dot{Q}_S^{CSs}$) in the SB and CSs channels of the Slice. This value must be equal to the power deposited because of the steady state conditions. Hence, once obtained \dot{Q}_S , the total BZR1 power \dot{Q}_{tot}^0 can be evaluated as:

$$\dot{Q}_{tot}^0 = \dot{Q}_S \frac{V_{NM} + V_{TC}}{V_S} = \dot{Q}_S \left(6 + \frac{V_{TC}}{V_S} \right) \quad (1)$$

Then, the total power exchanged in the NM part, \dot{Q}_{NM} , can be calculated along with the SB and CSs fractions:

$$\dot{Q}_{NM} = \dot{Q}_S \frac{V_{NM}}{V_S} \quad (2)$$

$$\dot{Q}_{NM}^{SB} = \dot{Q}_S \frac{V_{NM}^{SB}}{V_S} \quad (3)$$

$$\dot{Q}_{NM}^{CSs} = \dot{Q}_{NM} - \dot{Q}_{NM}^{SB} \quad (4)$$

Thus, the total BZR1 mass flow rate \dot{m}_{tot}^0 and the inlet temperature of the CSs in the modelled TC region are obtained as:

$$\dot{m}_{tot}^0 = \frac{\dot{Q}_{tot}^0}{c_p (T_{out}^{SB}|_{TARGET} - T_{in}^{CSs}|_{TOT})} \quad (5)$$

$$T_{in}^{CSs}|_{TC} = T_{in}^{CSs}|_{TOT} + \frac{\dot{Q}_{NM}^{CSs}}{c_p \dot{m}_{tot}^0} \quad (6)$$

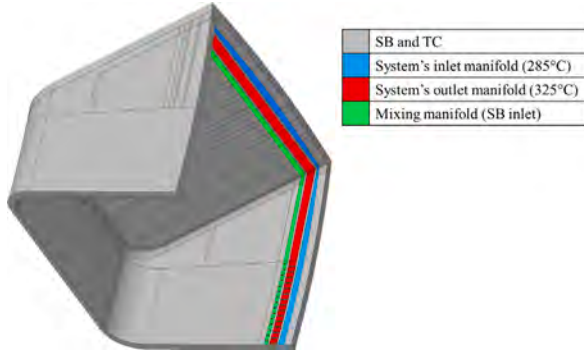


Fig. 9. Detail of the imposed temperature on the manifolds.

From \dot{m}_{tot}^0 , it is possible to obtain the flow rate per SB channel \dot{m}_{SB}^0 and per CS channel \dot{m}_{CSs}^0 :

$$\dot{m}_{SB}^0 = \frac{\dot{m}_{tot}^0}{n_{SB}} \quad (7)$$

$$\dot{m}_{CSs}^0 = \frac{\dot{m}_{tot}^0}{n_{CSs}} \quad (8)$$

Finally, the HTC values can be found using the Nusselt number, derived from Gnielinski correlation [6]:

$$HTC_{SB}^0 = \frac{Nu_{SB}^0 K}{D_h} \quad (9)$$

$$HTC_{CSs}^0 = \frac{Nu_{CSs}^0 K}{D_h} \quad (10)$$

Once obtained the flow rates, the HTCs and the inlet temperature of the CSs, the thermal analysis of the TC region can be performed and the power exchanged in SB and CSs can be obtained so that:

$$\dot{Q}_{SB}^1 + \dot{Q}_{CSs}^1 + \dot{Q}_{NM}^1 = \dot{Q}_{tot}^1 \quad (11)$$

At this point, \dot{Q}_{tot}^1 can be compared with \dot{Q}_{tot}^0 . The described procedure is iterated until $\dot{Q}_{tot}^{n+1} \approx \dot{Q}_{tot}^n$. Moreover, it is also necessary, for every iteration, to check if the weighted average ($\bar{T}_{out|tot}^{SB}$) between the average temperature of the coolant exiting the TC SB ($\bar{T}_{out|TC}^{SB}$), obtained from the thermal analysis, and the average temperature of the coolant exiting the NM SB ($\bar{T}_{out|NM}^{SB}$) converge to the design value of 325 C. In this regard, $\bar{T}_{out|NM}^{SB}$ and $\bar{T}_{out|tot}^{SB}$ are obtained as following:

$$\bar{T}_{out|NM}^{SB} = \bar{T}_{out}^{CSs} + \frac{\dot{Q}_{NM}^{SB}}{c_p \dot{m}_{SB} n_{NM}^{SB}} \quad (12)$$

$$\bar{T}_{out|tot}^{SB} = \frac{n_{TC}^{SB} \bar{T}_{out|TC}^{SB} + n_{NM}^{SB} \bar{T}_{out|NM}^{SB}}{n_{tot}^{SB}} \quad (13)$$

4.4. Manifolds

Regarding the manifolds, Dirichlet conditions has been imposed on the selected water-wetted surfaces (Fig. 9), in particular:

- temperature of the inlet manifolds set to 285 C;
- temperature of the outlet manifolds set to 325 C;
- temperature of the mixing manifold set to \bar{T}_{out}^{CSs} .

In particular, the last condition was implemented through the use of python scripts.

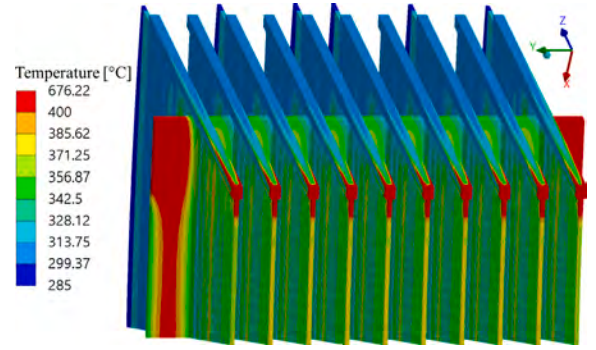


Fig. 10. TC ver.0 thermal field within CSs.

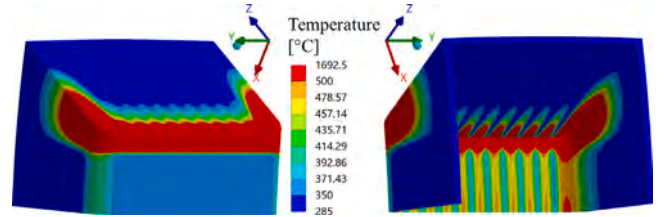


Fig. 11. TC ver.0 thermal field within SB and TC plate.

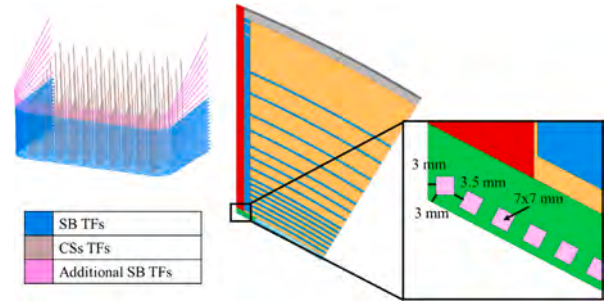


Fig. 12. WLCB TC ver.1 details.

5. WLCB top cap thermal analyses results

Once the boundary conditions have been properly assessed, temperature-dependent properties [7–10] of the materials considered were implemented. From this point, the actual design-by-analysis procedure begins, starting with the generation of the TC ver.0 Finite Element Method (FEM) model, reproducing Eurofer structural material, Tungsten, water, ACB and the Pb pool. Then, TC ver.0 thermal analysis has been carried out. The results, reported in Figs. 10 and 11 have shown that the thermal requirement has not been met yet. In fact, both in the SB and in the CSs the maximum temperature in the Eurofer structure is considerably higher than 550 C.

To overcome this issue, the TC ver.1 has been obtained by adding 8 FW channels within the FW-SW region with respect to the previous model, near the TC plate, as depicted in Fig. 12.

A new FEM model has then been generated and the thermal analysis has been carried out. The results, in terms of arising thermal field are reported in Figs. 13 and 14, respectively showing the temperature distribution within the SB, TC and CSs, highlight the need of further revisions.

In fact, the temperature of the TC plate and of some regions of the SB widely overcomes the limit of 550 C, underlining the necessity of a dedicated cooling system. Instead, thanks to the adopted design update, the temperature of the stiffeners stays well below the prescribed limit.

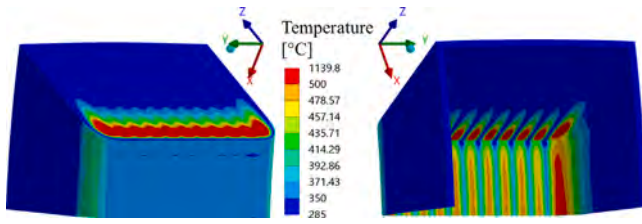


Fig. 13. TC ver.1. Thermal field within SB and TC plate.

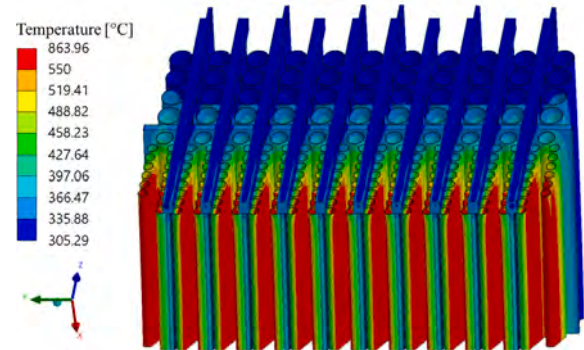


Fig. 17. TC ver.2. Thermal field within CSs and ACB tubes.

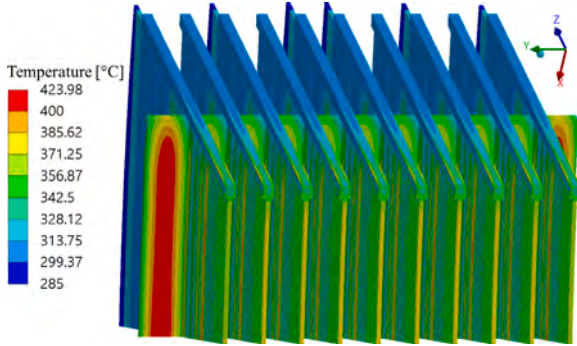


Fig. 14. TC ver.1. Thermal field within CSs.

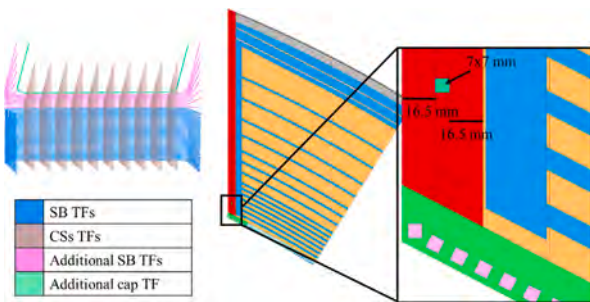


Fig. 15. WLCB TC ver.2 details.

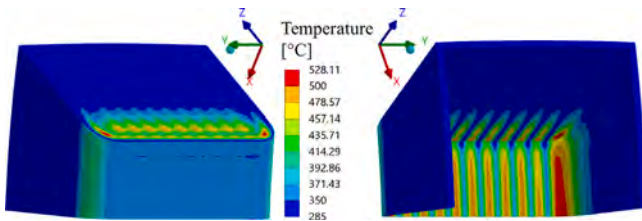


Fig. 16. TC ver.2. Thermal field within SB and Top Cap plate.

On the basis of the results previously obtained, a square channel, with a “U-shape” has been implemented to the model, as reported in Fig. 15, to adequately refrigerate the upper region, resulting in the TC ver.2.

After the generation of the new FEM model, the thermal analysis has been performed and the thermal fields arising within SB, TC, CSs and ACB tubes are reported in Figs. 16 and 17.

The considered further update allows reducing the temperature of the TC region below the prescribed limit for the structural material. Instead, paying attention to the ACB tubes, the temperature far exceeds the limit, reaching a maximum value of ≈ 860 C, due to the lack of refrigeration. This behaviour highlights the necessity of a deep design review of that region, possibly taking into account the option of substituting the tubes with other kinds of components. Anyway, since

Table 1

Cambiare.

Data	TC ver.0	TC ver.1	TC ver.2
SB channels	30	38	38
TC channels	0	0	1
Nodes $\times 10^6$	2.2	2.9	3.2
Elements $\times 10^6$	4	6.2	6.9
\dot{m}_{SB} [kg/s]	0.130	0.127	0.127
\dot{m}_{CSs} [kg/s]	0.197	0.199	0.200
HTC_{SB} [kW/(m ² C)]	29.98	29.4	29.3
HTC_{CSs} [kW/(m ² C)]	30.4	30.7	30.8
T_{in}^{CS} _{TC} [C]	303.2	303	303
\bar{T}_{out}^{CS} [C]	308	307.4	307.3
\bar{T}_{out}^{SB} _{TC} [C]	324.7	323.4	323.3
\bar{T}_{out}^{SB} _{NM} [C]	325.9	325.8	325.7

the ACB tubes have no structural role, the structural analysis of the TC ver.2 has been performed, not including them in the simulation. The characteristics of the FEM models used, the converged convective conditions and the main results of the analyses performed are summarized in Table 1.

6. WLCB TC ver.2 thermo-mechanical analysis

A thermo-mechanical analysis of the WLCB TC ver.2 geometric layout, aimed at investigating its structural behaviour in light of the RCC-MRx design criteria [11] in case of significant irradiation, has been performed. In particular, in analogy with what already done in the WCLL reference analyses, two steady-state loading scenarios have been investigated: the Normal Operation (NO) and the Over-Pressurization (OP). The first is related to the nominal operative condition, the other, conversely, to an off-normal condition derived from an in-box LOCA event, causing the sudden pressurization of the SB due to a leak of coolant.

6.1. The FEM model

The same FEM model used for the thermal analysis has been considered. In particular in Fig. 18 the details of the TC and SB mesh are shown.

The Pb, ACB tubes, ACB and water have not been included but their mechanical effect has been considered by means of proper loads. To reproduce the two selected loading scenarios a set of loads and boundary conditions has been considered. The non-uniform thermal field calculated from the thermal analysis has been applied onto the structure in order to consider the onset of thermal-induced (i.e. secondary) stress. Then, a pressure has been applied onto the water-wetted and Pb-wetted surfaces, to simulate their presence inside the SB. In particular, the design pressure value of 17.825 MPa has been assigned

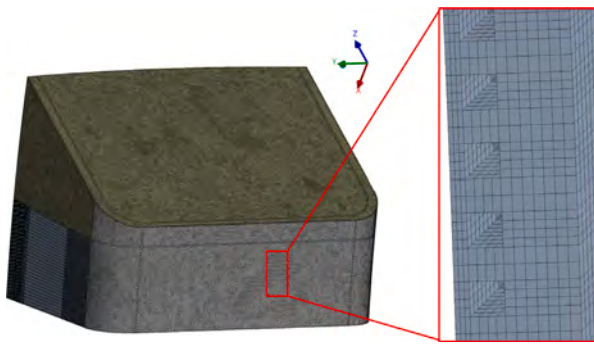


Fig. 18. Detail of the mechanical FEM model of TC ver.2.

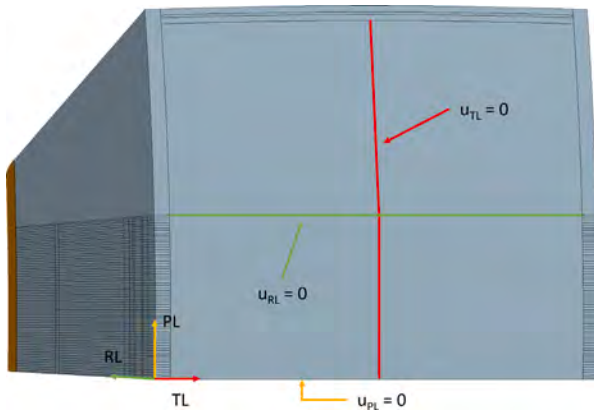


Fig. 19. Mechanical restraints considered in TC ver.2.

to the water-wetted surfaces both for the NO and the OP loading scenario [12]. On the other hand, with regard to the Pb, the design pressure value of 0.575 MPa has been considered for the NO, whereas the water pressure value (17.825 MPa) has been imposed for the OP loading scenario in order to simulate the sudden pressurization of the SB. Moreover, the gravitational load has been applied to the whole structure. Since neither the Pb, nor ACB, nor ACB tubes nor water have been modelled, a temperature-dependent Eurofer equivalent density has been calculated and applied to the structure, to simulate their weight, considering the corresponding material volumetric percentages. Then, to simulate the presence of the attachment system onto the TC region, displacements along the radial and toroidal directions of a local coordinate system have been prevented to two groups of nodes, as indicated in Fig. 19. Finally, the nodes corresponding to the bottom surface of the model have been constrained along the local poloidal direction to simulate the continuity of the segment [13,14].

6.2. Analysis and results

Steady-state structural analyses of the TC ver.2 have been performed under the NO and OP loading scenarios, to investigate its thermo-mechanical behaviour in view of the RCC-MRx criteria. The two investigated scenarios are classified as Level A (NO) and Level D (OP) of the structural design code. The results show that the most critical area, in terms of stresses, is the FW region, both in NO and in OP loading scenario. As an example, in Fig. 20 and in Fig. 21, the Von Mises stress fields, within the SB, TC and CSs under the NO and OP loading scenarios, are reported. As it can be observed, Von Mises stress values lower than 400 MPa are predicted for the most of the investigated domain. This result is quite encouraging in sight of the verification of the RCC-MRx criteria.

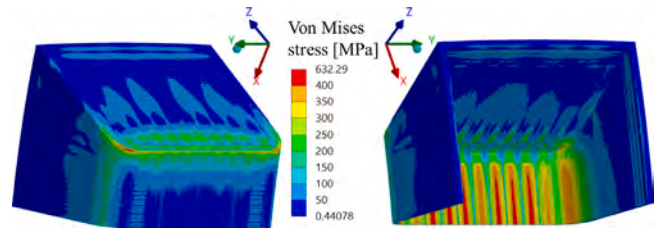


Fig. 20. TC ver.2. Von Mises stress field within SB and TC plate under NO loading scenario.

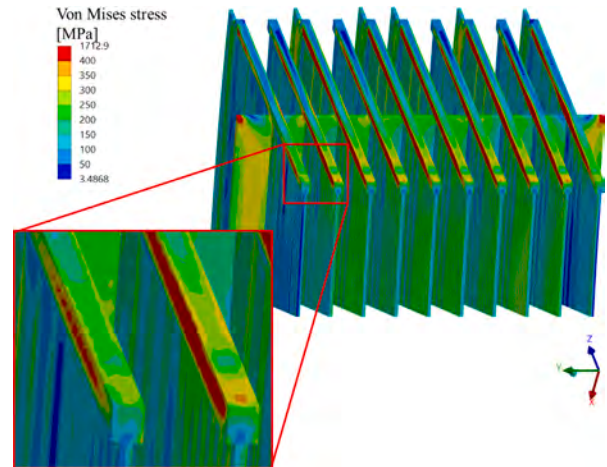


Fig. 21. TC ver.2. Von Mises stress field within CSs under OP loading scenario.

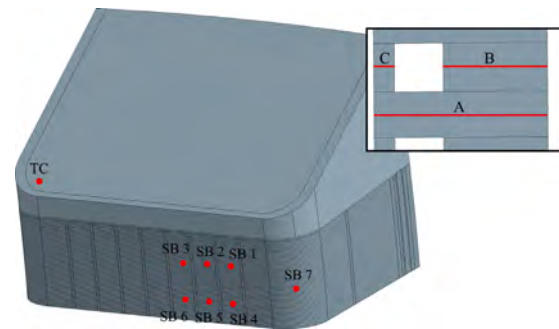


Fig. 22. Locations of the paths for SB and TC.

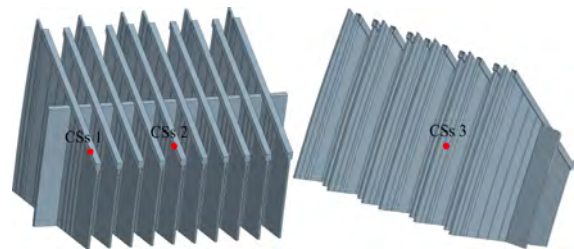


Fig. 23. Locations of the paths for CSs.

Therefore, a stress linearization procedure has been performed along a selected set of paths, whose locations are indicated in Figs. 22 and 23. It has to be noted that, as to SB paths, a triplet of paths has been created for each location, as shown in detail in Fig. 22. Then, in total, 25 paths belonging to SB, TC and CSs have been considered. Looking at the code, four criteria have been selected against: Immediate Excessive

Table 2
RCC-MRx structural criteria verification.

Path - load scenario	T_{ave} [C]	P_m/S_m	$(P_m + P_b)/(k_{eff} \cdot S_m)$	$(P_m + Q_m)/S_{em}$	$(P_m + P_b + Q + F)/(S_{et})$
CSs 1 - NO	311	0.74	0.52	1.39	0.36
CSs 2 - NO	312	0.88	0.66	1.15	0.28
CSs 3 - NO	325	1.44	0.97	1.05	0.25
CSs 1 - OP	311	0.79	0.60	1.13	0.37
CSs 2 - OP	312	1.14	0.76	0.98	0.29
CSs 3 - OP	325	0.65	0.44	0.57	0.16

Deformation (IED) expressed by the rule $P_m < S_m$, Immediate Plastic Instability (IPI) expressed by the rule $(P_m + P_b) < (k_{eff} \cdot S_m)$, Immediate Plastic Flow Localization (IPFL) expressed by the rule $(P_m + Q_m) < S_{em}$ and Immediate Fracture due to exhaustion of ductility (IF) expressed by the rule $(P_m + P_b + Q + F) < S_{et}$.

For the sake of brevity, the full set of results is not reported. The considered criteria have been largely matched in both the scenarios along the 21 paths belonging to SB as well as the TC region path. Also the IPFL criterion, which is normally the most critical in the DEMO BB design analysis, is widely fulfilled with ratios in between stress intensity and stress limit never achieving 0.6. The only paths not fully verifying the criteria are those located within the CSs, as reported in Table 2. Here, the values in red indicate the not-matched criteria whereas the values in orange mean that the criterion is met with a narrow margin (between 0.8 and 1). This behaviour can be attributable to the small thickness of the CSs collectors and it could be easily fixed by increasing it.

7. Conclusions

The thermo-mechanical behaviour of the TC region of the WLCB COB segment has been investigated in this paper. After a design by analysis procedure, carried out looking at the thermal requirement on the Eurofer maximum allowable temperature, the TC ver.2 configuration has been achieved. The thermal analysis of that configuration highlights the need to review the ACB tubes region, equipping them a suitable refrigeration system or replacing them with another kind of component, as the predicted temperature is considerably higher than the prescribed limit of 550 C in a wide region. Beyond this exception, the thermal requirement is largely met throughout the rest of the structural material. Therefore, considering that the tubes do not play any primary structural or safety role, a structural analysis of the TC ver.2 configuration has been performed. The RCC-MRx criteria are widely fulfilled in within the SB and the TC under both normal and off-normal loading scenarios. Instead, the verification fails within the CSs collectors, where the thickness needs to be increased. In conclusion, the obtained results are very promising and they have shown the existence of margins for further development of the WLCB concept, highlighting some issues that might be easily overcome. Hence, the study herein reported will pave the way for future and more refined analysis leading to the definition of a sound conceptual design of the WLCB BB system for DEMO.

List of acronyms

ACB	Advanced Ceramic Breeder
BB	Breeding Blanket
BZR	Breeder Zone Region
COB	Central Outboard Blanket
CS	Cooling Stiffener
DEMO	DEMOstration Power Plant
EU	European Union
FEM	Finite Element Method
FW	First Wall
HCPB	Helium-Cooled Pebble Bed
HTC	Heat Transfer Coefficient

IF	Immediate Fracture due to exhaustion of ductility
IED	Immediate Excessive Deformation
IPI	Immediate Plastic Instability
IPFL	Immediate Plastic Flow Localization
MFR	Mass Flow Rate
NM	Not Modelled
NO	Normal Operation
OP	Over-Pressurization
SB	Segment Box
SW	Side Wall
TC	Top Cap
WCLL	Water-Cooled Lead Lithium
WLCB	Water-Cooled Lead-Ceramic Breeder

CRediT authorship contribution statement

S. Giambrone: Conceptualization, Investigation, Methodology, Writing – original draft. **I. Catanzaro:** Conceptualization, Investigation, Methodology, Writing – original draft. **G. Bongiovi:** Conceptualization, Investigation, Methodology, Writing – original draft. **P.A. Di Maio:** Conceptualization, Investigation, Methodology, Writing – original draft. **E. Vallone:** Conceptualization, Investigation, Methodology, Writing – original draft. **P. Arena:** Conceptualization, Investigation, Methodology, Writing – original draft. **F.A. Hernández:** Conceptualization, Investigation, Methodology, Writing – original draft. **I. Moscato:** Conceptualization, Investigation, Methodology, Writing – original draft. **G.A. Spagnuolo:** Conceptualization, Investigation, Methodology, Writing – original draft. **P. Chiovaro:** Conceptualization, Investigation, Methodology, Writing – original draft. **M. Giardina:** Conceptualization, Investigation, Methodology, Writing – original draft. **A. Quartararo:** Conceptualization, Investigation, Methodology, Writing – original draft. **E. Tomarchio:** Conceptualization, Investigation, Methodology, Writing – original draft.

Declaration of competing interest

The authors declare that they have no known competing financial interests or personal relationships that could have appeared to influence the work reported in this paper.

Data availability

Data will be made available on request.

Acknowledgements

This work has been carried out within the framework of the EUROfusion Consortium, funded by the European Union via the Euratom Research and Training Programme (Grant Agreement No 101052200 — EUROfusion). Views and opinions expressed are however those of the author(s) only and do not necessarily reflect those of the European Union or the European Commission. Neither the European Union nor the European Commission can be held responsible for them.

References

- [1] L.V. Boccaccini, et al., Status of maturation of critical technologies and systems design: Breeding blanket, *Fusion Eng. Des.* 179 (2022) 113116, <http://dx.doi.org/10.1016/j.fusengdes.2022.113116>.
- [2] G. Zhou, et al., A water cooled Lead Ceramic Breeder blanket for European DEMO, *Fusion Eng. Des.* 168 (2021) 112397, <http://dx.doi.org/10.1016/j.fusengdes.2021.112397>.
- [3] A. Gioè, et al., Thermomechanical and thermo-fluid-dynamic coupled analysis of the top cap region of the water-cooled lithium lead breeding blanket for the EU DEMO fusion reactor, *Energies* 16 (7) (2023) <http://dx.doi.org/10.3390/en16073249>.
- [4] P. Arena, et al., The demo water-cooled lead–lithium breeding blanket: Design status at the end of the pre-conceptual design phase, *Appl. Sci. (Switzerland)* 11 (24) (2021) <http://dx.doi.org/10.3390/app112411592>.
- [5] P. Pereslvtsev, et al., Neutronic activity for development of the promising alternative water-cooled DEMO concepts, *Appl. Sci.* 13 (13) (2023) <http://dx.doi.org/10.3390/app13137383>.
- [6] V. Gnielinski, New equations for heat and mass transfer in turbulent pipe and channel flow, *Int. Chem. Eng.* 16 (2) (1976) 359–368.
- [7] E. Gaganidze, *Materials Properties Handbook - EUROFER97*, EUROfusion IDM Ref.: 2NZHBS v1.3, 2023.
- [8] E. Gaganidze, et al., *Materials Properties Handbook - Tungsten*, EUROfusion IDM Ref.: 2P3SPL v1.0, 2020.
- [9] S. Papeschi, et al., *Study of Thermal Conductivity of Ceramic Pebble Beds – 3rd Intermediate Technical Note* (2016), EUROfusion IDM Ref.: 2N8Y27 v1.1, 2020.
- [10] OECD and Nuclear Energy Agency, *Handbook on lead-bismuth eutectic alloy and lead properties, materials compatibility, thermalhydraulics and technologies*, 2015, <http://dx.doi.org/10.1787/42dcd531-en>.
- [11] AFCEN, *RCC-MRx, design and construction rules for mechanical components of nuclear installations*, 2013.
- [12] G. Spagnuolo, et al., Development of load specifications for the design of the breeding blanket system, *Fusion Eng. Des.* 157 (2020) 111657, <http://dx.doi.org/10.1016/j.fusengdes.2020.111657>.
- [13] P.A.D. Maio, et al., On the effect of stiffening plates configuration on the DEMO Water Cooled Lithium Lead Breeding Blanket module thermo-mechanical behaviour, *Fusion Eng. Des.* 146 (2019) 2247–2250, <http://dx.doi.org/10.1016/j.fusengdes.2019.03.163>.
- [14] P.A.D. Maio, et al., Analysis of the thermo-mechanical behaviour of the DEMO Water-Cooled Lithium Lead breeding blanket module under normal operation steady state conditions, *Fusion Eng. Des.* 98–99 (2015) 1737–1740, <http://dx.doi.org/10.1016/j.fusengdes.2015.03.051>.